

## Magnetic minibands in lateral semiconductor superlattices

This article has been downloaded from IOPscience. Please scroll down to see the full text article.

1992 *J. Phys.: Condens. Matter* 4 7355

(<http://iopscience.iop.org/0953-8984/4/36/010>)

[View the table of contents for this issue](#), or go to the [journal homepage](#) for more

Download details:

IP Address: 171.66.16.96

The article was downloaded on 11/05/2010 at 00:30

Please note that [terms and conditions apply](#).

# Magnetic minibands in lateral semiconductor superlattices

Helmut Silberbauer

Institut für Theoretische Physik, Universität Regensburg, D-8400 Regensburg, Federal Republic of Germany

Received 8 June 1992

**Abstract.** A new quantum mechanical method for calculating the miniband structure of lateral surface superlattices in a perpendicular magnetic field is developed. The Schrödinger equation is solved via expansion in a basis that is well adapted both to the translational symmetry of the problem and the magnetic field. The approach is quite similar to the nearly-free-electron approximation in the zero-field case and is capable of dealing with arbitrary potential shapes.

## 1. Introduction

During the past few years advances in submicron lithography have made it possible to prepare lateral superlattices on the surface of high-mobility two-dimensional electron systems with lattice constants of a few hundred nanometres [1]. With mean free paths of the order of several microns the electrons in these systems may exhibit transport properties that are due to the periodic potential rather than to processes of scattering by lattice imperfections. As an additional parameter for transport experiments a magnetic field is frequently applied perpendicular to the lateral superlattice. It introduces the cyclotron length as a characteristic tunable length scale, which in the interplay with the lattice constant is expected to result in typical modifications of the quantum mechanical properties.

Experimentally lateral superlattices have been fabricated by several groups using different techniques for imposing different kinds of periodic structures. One limit, the formation of isolated electron systems confined in all three dimensions, the so-called 'quantum dots', is in general well understood [2]. But if one alters the experimental conditions such that the barriers between adjacent dots become lower and the dots get coupled more complex features are observed [3]. Also the complementary situation, a repulsive potential, leading to 'anti-dots', instead of attractive potential 'islands' in the case of the dots, has been realized [4].

The far-infrared experiments [3, 4], which show a characteristic two-peak structure of dipole-allowed transitions  $\omega_{\pm}$  for parabolic quantum dots, exhibit the nature of the lateral potential by deviations from this behaviour. Naturally, this can be quite different for dot and antidot arrays and may also depend on the preparation of the lateral structure. Deviations of the magnetoconductivity from the usual SDH-oscillations for the homogeneous electron system [5] have been interpreted by concepts of non-linear classical dynamics in the low-field case [6] or by quantum transport due to formation of subbands within each Landau level in the high-field case [7]. The latter has been taken as an indication of Hofstadter's butterfly [8].

Theoretical studies of electrons subject to both a magnetic field and a periodic potential have in fact a long history [9]. However, because those studies were directed towards the more principal aspects of the problem, they have often been based on very simple shapes of the periodic potential, like  $V(x, y) = V_1 \cos(Kx) + V_2 \cos(Ky)$ .

Unfortunately the shape of the potential in real systems is not known. Therefore it seems desirable to have a method applicable to a wide range of different potentials. The method developed in this paper is capable of dealing with arbitrary shapes of the periodic potential. The Schrödinger equation is solved by expanding the solution in a basis of symmetry-adapted basis functions. Those functions are not the magnetic Wannier functions, which have often been used in the literature [9], but eigenfunctions to the basic magnetotranslations [10] of the lattice.

## 2. The Hamiltonian

Experimentally, lateral superlattices are often realized by etching and/or gate techniques. The main effect of both techniques is that they alter the energy of the bottom of the conduction band by surface and/or electrostatic band bending periodically in the  $x$ - $y$ -plane. This results in a position dependence of the subband energies of the underlying heterostructure, described by a phenomenological potential  $V(x, y)$ .  $V(x, y)$  is periodic, with  $l_1$  and  $l_2$  being the primitive translations of the corresponding Bravais lattice  $\mathcal{B}$ :

$$V(\mathbf{r} + ml_1 + nl_2) = V(\mathbf{r}) \quad n, m \text{ integer.}$$

By taking this approach, it is assumed that the electron motion in the  $x$ - $y$ -plane is decoupled from the motion in the  $z$ -direction. This assumption is justified if the lateral potential is weak compared with the confining potential of the heterostructure, i.e. only the lowest subband due to the  $z$ -confinement is occupied. Going beyond this approximation would require a complete, self-consistent solution of both the three-dimensional Schrödinger and the Poisson equation with appropriate boundary conditions, e.g. for a gate. This has been done for a single isolated quantum dot [11], but is at present numerically too difficult for periodic structures.

Moreover the electron spin and all band structure effects beyond the effective mass approximation are neglected. Thus lateral superlattices are described by the Hamiltonian

$$H = (1/2m^*)(\mathbf{p} + (e/c)\mathbf{A})^2 + V(x, y). \quad (1)$$

The magnetic field is applied perpendicular to the electron plane and the symmetric gauge for the vector potential is used:

$$\mathbf{A} = (B/2)(-y, x, 0). \quad (2)$$

Finally all lengths are normalized with respect to the cyclotron length ( $\lambda_c \equiv 1$ ) and by introducing the usual inter- and intra-Landau-level ladder operators  $a$  and  $b$ , the Hamiltonian may be written as

$$H = \hbar\omega_c^*(a^\dagger a + \frac{1}{2}) + V(a, b). \quad (3)$$

The dependence of the potential on the  $b$ -operator indicates the removal of the Landau level degeneracy due to the lateral superlattice.

### 3. Magnetotranslations

In the presence of a magnetic field, translations in the  $x$ - $y$ -plane do not commute with the kinetic energy operator. But if the field is homogeneous, they obviously map the physical system back onto itself, and in fact they are just gauge transformations. To get an operator which represents that symmetry by commuting with the kinetic energy, one has to compose a translation with the inverse of the corresponding gauge transformation:

$$S(\mathbf{R}) = \exp((1/\sqrt{2})(R^*b - Rb^\dagger)) = \exp((i/2)(\mathbf{R} \times \mathbf{r}) \cdot \hat{z})T(\mathbf{R})$$

with  $T(\mathbf{R})\psi(\mathbf{r}) = \psi(\mathbf{r} + \mathbf{R}).$  (4)

The unitary operators  $S$  are called magnetotranslations and have been discussed in detail elsewhere [10].

In general magnetotranslations, in contrast to ordinary translations, do not commute with each other. One easily shows the relation

$$[S(\mathbf{R}_1), S(\mathbf{R}_2)] = 0 \iff |\mathbf{R}_1 \times \mathbf{R}_2| = 2\pi u \quad \text{with } u \text{ integer.} \quad (5)$$

Physically  $u$  counts the number of flux quanta through the parallelogram defined by  $\mathbf{R}_1$  and  $\mathbf{R}_2$ . For a superlattice system with basic translations  $\mathbf{l}_1$  and  $\mathbf{l}_2$  this means that we have to restrict ourselves to magnetic fields, which fulfil (in SI units)

$$B = [h/(e|\mathbf{l}_1 \times \mathbf{l}_2|)]g_l \quad \text{with } g_l \text{ integer.} \quad (6)$$

In practice this is not very restricting, because for usual lattice parameters the spacing between allowed field values is small and can be made smaller by choosing a larger unit cell instead of the elementary cell of the lattice.

Now one can establish the commutation relations for the basic magnetotranslations of the lattice:

$$[S(\mathbf{l}_1), S(\mathbf{l}_2)] = [S(\mathbf{l}_1), H] = [S(\mathbf{l}_2), H] = 0. \quad (7)$$

Because of the unitarity of the magnetotranslations, all eigenvalues are of modulus one and the eigenvalue equations may be written as

$$S(\mathbf{l}_1)\psi = e^{i\Theta_1}\psi \quad S(\mathbf{l}_2)\psi = e^{i\Theta_2}\psi. \quad (8)$$

Because of (7) they can be solved simultaneously and the solutions for fixed  $\Theta_1$  and  $\Theta_2$  form a Hilbert space  $H(\Theta_1, \Theta_2)$ . Since the two primitive magnetotranslations commute with the Hamiltonian, the eigenfunctions of the Hamiltonian can be chosen in such a way that they belong to one of the  $H(\Theta_1, \Theta_2)$ . Therefore it is sufficient to solve the Schrödinger equation in each Hilbert space  $H(\Theta_1, \Theta_2)$  separately. The two phases  $\Theta_1$  and  $\Theta_2$  play a role analogous to the  $\mathbf{k}$ -vector in the zero-field case. Energy levels exhibit a two-dimensional dispersion  $E(\Theta_1, \Theta_2)$ . Obviously it is sufficient to restrict the range of  $\Theta_1$  and  $\Theta_2$  to the interval  $[-\pi, \pi]$ , the first quasi-Brillouin zone.

#### 4. Symmetry-adapted functions

We look for a basis of  $H(\Theta_1, \Theta_2)$ , where all elements are also eigenfunctions of the kinetic part of the Hamiltonian (3). This basis is then well adapted both to the translational symmetry and the presence of a magnetic field in the problem.

We use the set of functions proposed by Ferrari [12]. The integer  $g_l$  defined in equation (6) has to be factored into  $g_l = pq$ . Then a finer lattice than the original Bravais lattice is defined by

$$c = l_1/p \quad \text{and} \quad d = l_2/q.$$

In this finer lattice the magnetic flux through one unit cell is precisely one flux quantum. We further define

$$\phi_{n_L}^{n_1, n_2}(\mathbf{r}) = (pq)^{-1/2} \sum_{m, n=-\infty}^{\infty} [S(c)e^{-im}]^m [S(d)e^{-in}]^n \phi_{n_L}(\mathbf{r}) \quad (9)$$

with

$$\begin{aligned} \mu &= (1/p)(\theta_1 + 2\pi n_1) & \text{and} & \nu = (1/q)(\theta_2 + 2\pi n_2) \\ n_1 &\in I_1 = \{0, \dots, p-1\} & \text{and} & n_2 \in I_2 = \{0, \dots, q-1\} \\ n_L &\in \{0, 1, 2, 3, \dots\}. \end{aligned}$$

$\phi_{n_L}$  is a Landau eigenfunction defined by  $a^\dagger a \phi_{n_L} = n_L \phi_{n_L}$  and  $b \phi_{n_L} = 0$ .

Since magnetotranslations only involve the  $b$  ladder operators,  $\phi_{n_L}^{n_1, n_2}$  is also an eigenfunction of the number operator  $a^\dagger a$ :

$$a^\dagger a \phi_{n_L}^{n_1, n_2} = n_L \phi_{n_L}^{n_1, n_2} \quad (10)$$

and therefore of the kinetic energy.

The functions  $\phi_{n_L}^{n_1, n_2}$  form a complete, orthogonal set of functions in  $H(\Theta_1, \Theta_2)$ , provided that  $(\mu, \nu) \neq (\pi, \pi)$  for all  $(n_1, n_2) \in I_1 \times I_2$ . Their norm may easily be evaluated as

$$\|\phi_{n_L}^{n_1, n_2}\|^2 = \sum_{m, n=-\infty}^{\infty} (-1)^{nm} e^{i(\mu m + \nu n)} \exp(-\frac{1}{4}|nc + md|^2). \quad (11)$$

By defining

$$\psi_{n_L}^{n_1, n_2} := \|\phi_{n_L}^{n_1, n_2}\|^{-1} \phi_{n_L}^{n_1, n_2}.$$

an orthonormal basis in  $H(\Theta_1, \Theta_2)$  has been found.

## 5. Solution of the Schrödinger equation

The Schrödinger equation is solved by expanding the solutions in the basis  $\{\psi_{n_L}^{n_1, n_2}\}$  in  $H(\Theta_1, \Theta_2)$ . The numerical crucial point in this method is the evaluation of the matrix elements of the periodic potential in the given basis. This has been done to a great extent analytically, thus reducing the integration to summations of rapidly convergent series.

To take full advantage of the translational symmetry, the periodic potential is expanded in a Fourier series

$$V(\mathbf{R}) = \sum_{\mathbf{G} \in \mathcal{R}} v(\mathbf{G}) e^{i\mathbf{G} \cdot \mathbf{R}}$$

where  $\mathcal{R}$  is the reciprocal lattice to  $\mathcal{B}$ . What is then left to do is to calculate the matrix elements  $\langle n'_1, n'_2, n'_L | e^{i\mathbf{G} \cdot \mathbf{R}} | n_1, n_2, n_L \rangle$ , where  $\mathbf{G}$  is a reciprocal-lattice vector. After some algebra it becomes clear that these matrix elements vanish, unless there exist two integers  $M$  and  $N$  for which the following relations hold ( $\mathbf{G} = G_1 \hat{g}_1 + G_2 \hat{g}_2$  with  $\hat{g}_1, \hat{g}_2$  primitive translations of  $\mathcal{R}$ ):

$$G_1 = n'_1 - n_1 - Mp \quad (12)$$

$$G_2 = n'_2 - n_2 - Nq. \quad (13)$$

The non-vanishing matrix elements evaluate to

$$\begin{aligned} \langle n'_1, n'_2, n'_L | e^{i\mathbf{G} \cdot \mathbf{r}} | n_1, n_2, n_L \rangle \\ = G^{n'_L, n_L}(G) T_{n'_1, n'_2}^{n'_1, n'_2}(G) e^{-(1/4)|G|^2} / (\|\phi_{n'_L}^{n'_1, n'_2}\| \|\phi_{n_L}^{n_1, n_2}\|) \end{aligned}$$

with

$$T_{n'_1, n'_2}^{n'_1, n'_2}(G) = \sum_{\Lambda, \Omega = -\infty}^{+\infty} (-1)^{\Lambda \Omega} e^{i(\mu' \Lambda + \nu' \Omega)} e^{(i/2)G(\Lambda c + \Omega d)^*} e^{-(1/4)|\Lambda c + \Omega d|^2} \quad (14)$$

and

$$G^{n, m}(G) = \begin{cases} \sqrt{m! / n!} e^{-(1/4)|G|^2} (iG^*/\sqrt{2})^{n-m} L_m^{n-m}(|G|^2/2) : & n \geq m \\ \sqrt{n! / m!} e^{-(1/4)|G|^2} (iG/\sqrt{2})^{m-n} L_n^{m-n}(|G|^2/2) : & m \geq n. \end{cases}$$

In the above equations complex notation is used for two-dimensional vectors.

## 6. Results and discussion

To show the flexibility of the method, calculations for three different systems have been done. The model potentials, shown in figure 1, are chosen in such a way that

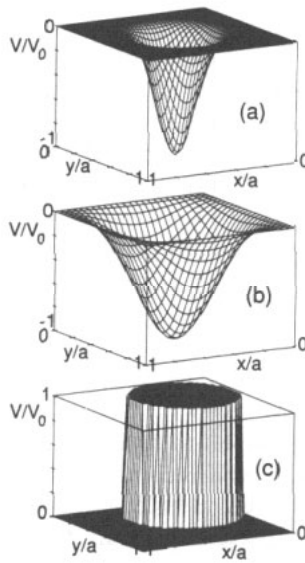


Figure 1. Effective potentials used for modelling arrays of (a) isolated quantum dots, (b) coupled quantum dots and (c) antidots. One elementary cell of the quadratic lattice is shown, the lattice constant is taken to be 500 nm, the potential depth 5 meV. In (c) the ratio of antidot diameter to lattice constant is  $\frac{2}{3}$ .

the systems may be regarded as arrays of isolated quantum dots, weakly coupled quantum dots and antidots, respectively.

For the calculations the effective mass of GaAs ( $m^* = 0.0665$ ), a quadratic unit cell for the lattice with side length  $a = 500$  nm and a potential depth  $V_0$  of 5 meV have been used. These assumptions are realistic in shallow mesa-etched samples [13].

For the isolated quantum dots (figure 1(a)) the miniband structure for three values of the magnetic field has been calculated and the results are shown in figure 2. For low magnetic fields the spectrum consists of some discrete levels below the lowest 2D Landau level and a quasi-continuous spectrum above. This is consistent with the results obtained by using a split operator technique on the solution of the time-dependent Schrödinger equation [14].

The discrete levels correspond to the energy levels of a strictly parabolic dot with the same curvature in the minimum. They exhibit no dispersion in  $\Theta$ , because they are closely bound in the dot and the wavefunctions of electrons in adjacent dots do not overlap. For the minibands in the quasi-continuum, however, dispersion is clearly observed at low fields. Their eigenstates are extended, due to overlap between neighbouring cells.

At higher magnetic fields the levels in the quasi-continuum cluster nearer and nearer to the 2D Landau levels. This is due to reduced Landau level mixing because of the wider spacing between adjacent Landau levels and increasing localization of the electrons in the magnetic field, which leaves more and more states in regions unaffected by the potential. Increasing localization resulting in a decrease of the overlap between neighbouring cells is also responsible for the vanishing dispersion at higher fields.

The dependence of the energy levels on the magnetic field for a fixed point near the  $\Gamma$ -point of the quasi-Brillouin zone is plotted in figure 3. In this plot one clearly sees the dot like behaviour of the discrete states and the clustering of the quasi-continuous level spectrum near the 2D Landau levels. At higher magnetic fields the

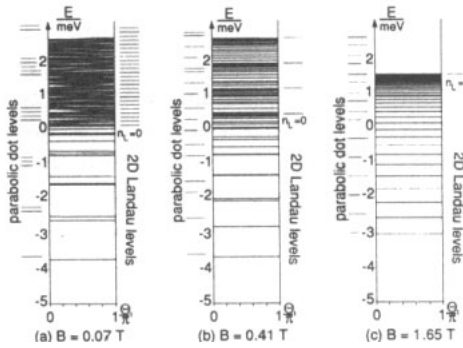


**Figure 2.** Magnetic minibands for the isolated dot system at three different values of the magnetic field. The dispersion is plotted along the  $\Theta_1$ -axis in the 2D quasi-Brillouin zone. To the left are the energy levels of a parabolic dot with the same curvature in the minimum plotted, to the right the Landau levels for  $V = 0$ .

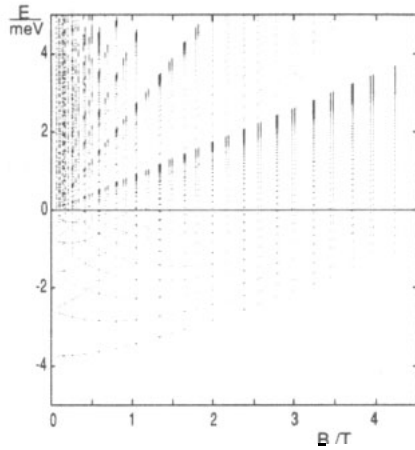


**Figure 3.** Magnetic field dependence of the energy levels of the isolated dot system at a fixed point ( $\Theta_1 = \Theta_2 = 0.3$ ) near the  $\Gamma$ -point.

spectrum is reminiscent of donors in a magnetic field [15].

As a second example the miniband structure of a coupled quantum dot system (figure 1(b)) has been calculated. The qualitative nature of the spectrum (figure 4) is quite similar to that of the isolated dots. The main difference is that dispersion is stronger and level clustering is much weaker in this case. Since the magnitude of the perturbation by the periodic potential depends on the potential height, averaged over one unit cell, this behaviour is intuitively clear.

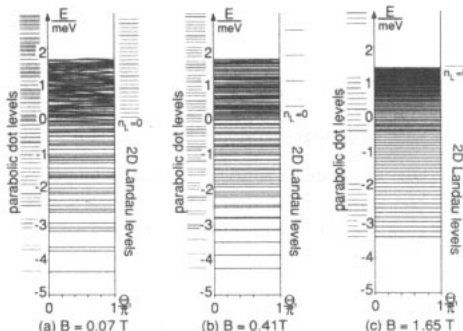


**Figure 4.** Magnetic minibands for the coupled dot system at three different values of the magnetic field. The dispersion is plotted along the  $\Theta_1$ -axis in the 2D quasi-Brillouin zone.

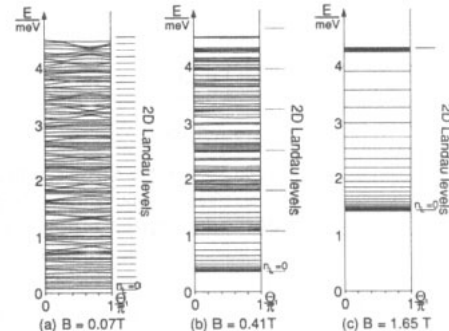


**Figure 5.** Magnetic minibands for the antidot system at three different values of the magnetic field. The dispersion is plotted along the  $\Theta_1$ -axis in the 2D quasi-Brillouin zone.

The last example is an array of circular antidots of finite height (figure 1(c)). In

in this case the energy levels are shifted from the 2D Landau levels to higher energies (figure 5) and the minibands exhibit a strong dispersion at low magnetic field. With increasing magnetic field the minibands become flat and cluster around the 2D Landau levels. This is for the same reason as in the case of the dots.

We now look at some eigenstates of the antidot system and compare them with classical trajectories, which are often discussed in this context [4, 6]. Of course there is no 1:1-mapping between eigenstates of the Hamiltonian in quantum mechanics and the trajectories of the corresponding classical system, because one has to form wave packets out of the eigenstates, which are no longer eigenstates of the Hamiltonian. Nevertheless plotting the probability density and probability current gives an idea of the nature of the eigenstates, which may then be related to classical trajectories.

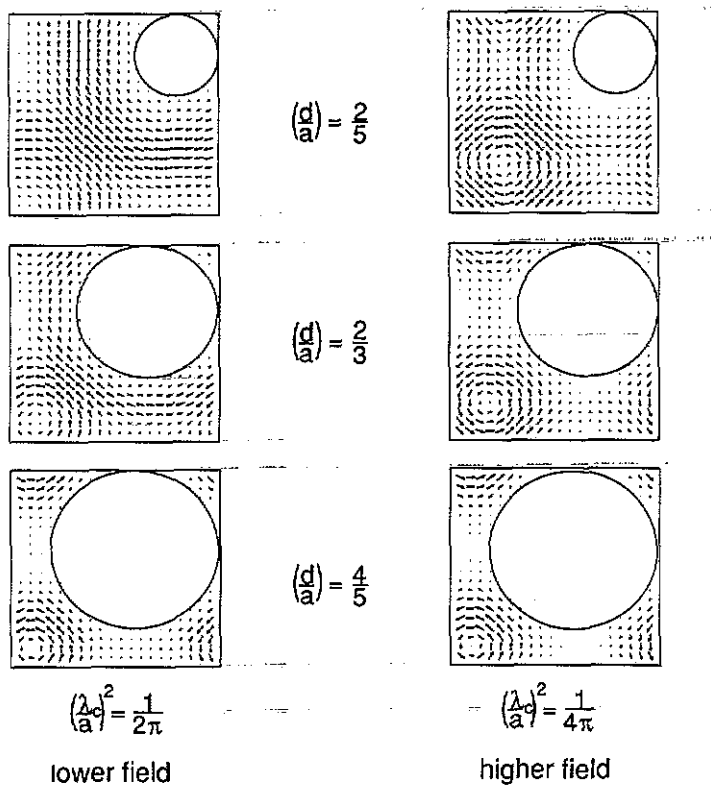


Figure 6. Probability current of the ground state for different ratios of cyclotron length  $\lambda_c$ , lattice constant  $a$  and antidot diameter  $d$ . The current is plotted inside one elementary cell of the lattice, the regions of non-vanishing potential are indicated by circles. The ground state has been calculated for  $\Theta_1 = \Theta_2 = 0.3$ .

Of particular interest is the question of whether electrons in the lowest miniband are circulating between four antidots or around a single antidot. It is connected with the interplay of three lengths: cyclotron length  $\lambda_c$ , lattice constant  $a$  and antidot diameter  $d$ . Classically it is expected that in low magnetic fields the electron circulates round a single antidot, whereas in high fields it is localized between four antidots. In the quantum mechanical picture the situation is less clear, but a fingerprint of the classical behaviour is found, too. In figure 6 the probability current for different ratios of  $\lambda_c/a$  and  $d$  is plotted. Comparing the situation for different ratios  $\lambda_c/a$  we

notice a strong probability current component along the antidot for the lower-field case (left-hand column in figure 6). In the higher field (right-hand column in figure 6) the probability current is just circulating between four antidots, corresponding to an electron on a cyclotron orbit located between the antidots. For values of  $d/a$  near one, where the channels between the electrons are nearly pinched off, the current for both fields is located between four antidots (last row in figure 6).

Finally two typical wavefunctions of higher minibands are plotted in figure 7. The upper one may be related to electrons skipping between the dots and the lower one is typical for higher states localized between four antidots.

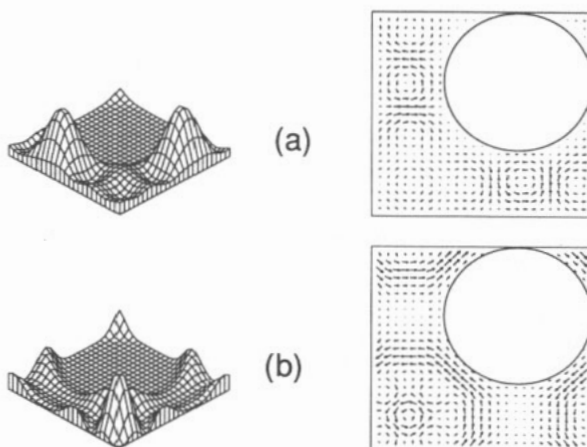


Figure 7. Probability density and probability current for states with higher miniband index: (a)  $n_{MB} = 5$  and (b)  $n_{MB} = 10$ . The states have been calculated for ( $\Theta_1 = \Theta_2 = 0.3$ ), the magnetic field strength here is 0.15 T. One elementary cell of the lattice is plotted, the antidots are again indicated by circles.

In conclusion, in this paper a method for calculating the energy spectrum and eigenstates of lateral surface superlattices in a perpendicular magnetic field has been developed. The method, which is not restricted to a special shape of the superlattice potential, has been applied to lattices of isolated quantum dots, coupled quantum dots and antidots. For comparison with experimental data it represents a flexible method for calculating the response functions.

### Acknowledgments

Stimulating discussions with Professor Ulrich Rössler are gratefully acknowledged. This work was sponsored by Deutsche Forschungsgemeinschaft, SFB 348.

### References

- [1] See review articles by
  - Weiss D 1991 *Festkörperprobleme (Advances in Solid State Physics 31)* ed U Rössler (Braunschweig: Vieweg)
  - Beenakker C W J and van Houten H 1991 *Solid State Physics* vol 44, ed H Ehrenreich and D Turnbull (New York: Academic)

- [2] Merkt U 1991 *Phys. Bl.* **47** 591
- [3] Lorke A, Kotthaus J P and Ploog K 1990 *Phys. Rev. Lett.* **64** 2559
- [4] Lorke A, Kotthaus J P and Ploog K 1991 *Superlatt. Microstruct.* **9** 103  
Kern K, Heitmann D, Grambow P, Zhang Y H and Ploog K 1991 *Phys. Rev. Lett.* **66** 1618
- [5] Smith C G *et al* 1990 *J. Phys.: Condens. Matter* **2** 3405  
Ensslin K and Petroff P M 1990 *Phys. Rev. B* **41** 12307  
Lorke A, Kotthaus J P and Ploog K 1991 *Phys. Rev. B* **44** 3447  
Yamashiro T *et al* 1991 *Solid State Commun.* **79** 885  
Weiss D, Roukes M L, Menschig A, Grambow P, von Klitzing K and Weimann G 1991 *Phys. Rev. Lett.* **66** 2790
- [6] Fleischmann R, Geisel T and Ketzmerick R 1992 *Phys. Rev. Lett.* **68** 1367
- [7] Gerhardt R R, Weiss D and Wulf U 1991 *Phys. Rev. B* **43** 5192  
Gerhardt R R and Pfannkuche D 1992 *Surf. Sci.* **263** 324
- [8] Hofstadter D 1976 *Phys. Rev. B* **14** 2239
- [9] See review articles by  
Fischbeck H J 1970 *Phys. Status Solidi* **38** 11  
Nenciu G 1991 *Rev. Mod. Phys.* **63** 91
- [10] Brown E 1964 *Phys. Rev. A* **133** 1038  
Zak J 1964 *Phys. Rev. A* **134** 1602  
Zak J 1964 *Phys. Rev. A* **134** 1607
- [11] Kumar A, Laux S E and Stern F 1990 *Phys. Rev. B* **42** 5166
- [12] Ferrari R 1990 *Phys. Rev. B* **42** 4598
- [13] Berthold *et al* 1992 *Phys. Rev. B* **45** 11350
- [14] Degani M H and Leburton J P 1992 *Superlatt. Microstruct.* **11** 79
- [15] Wagner H P and Prett W 1988 *Solid State Commun.* **66** 367